

Supplemental Information

Materials and Methods

MEF medium

MEF medium consists of Iscove's modified Dulbecco medium (IMDM) containing 10% iron-supplemented calf serum (Hyclone), with additional non-essential amino acids, GlutaMAX™, gentamycin, and beta-mercaptoethanol.

Fibroblast cultures from specific organs

Embryos from VEGF-GFP transgenic mice were harvested at 18.5 days post-coitus and dissected with micro-scissors under low power microscopy. The organs were minced, trypsinized for 20 minutes and seeded into T-25 cell culture dishes in 10 mL MEF medium as described above. The cells were split at 1:2-1:3 ratios when freshly confluent, passaged 2-4 times, then frozen or expanded for further studies.

Cell sorting

Cultures of primary fibroblasts at early passages were harvested by trypsinization, washed in phosphate buffered saline (PBS, 137 mM NaCl, 2.7 mM KCl, 10 mM Na₂HPO₄, 1.8 mM KH₂PO₄), filtered through a 70 μm cell strainer, and re-suspended in PBS at 10⁸ cells/mL. Cells were sorted by a MoFlo fluorescence activated cell sorter (Cytomation) and populations were collected into tubes containing complete MEF media. The sorted cells were immediately seeded into cell culture dishes and expanded. The purity of the resulting populations was confirmed by cytometry. Sorting was performed by the Flow Cytometry Core at the Schepens Eye Research Institute, Harvard Medical School.

Electron microscopy

Primary mouse embryonic cells were cultured to 90% confluence, fixed in Karnovsky solution (4% paraformaldehyde, 5% glutaraldehyde, 80 mM sodium cacodylate pH 7.4)

solution and stored in 0.2 M sodium cacodylate buffer pH 7.4. They were then post-fixed in osmium tetroxide, stained en bloc with uranyl acetate, dehydrated in graded ethanol solutions, infiltrated with propylene oxide/epoxy resin, and embedded in epoxy resin. Thin 1 μm sections were cut, stained with toluidine blue and examined by light microscopy or stained with lead citrate and examined in a Philips 301 electron microscope.

Colony isolation

MEFs were prepared from E18.5 VEGF-GFP mouse embryos. 5000-7000 cells freshly explanted from embryos were seeded in 15 cm culture dishes in MEF cell culture medium containing 20% iron-supplemented calf serum (Hyclone) and allowed to grow for 6-8 weeks with frequent change of MEF cell culture medium. Isolated cell clones with normal morphology were picked under a microscope and plated into 96-well microplates. The picked colonies were expanded and the serum percentage was gradually reduced to 10% during the expansion.

***In vitro* differentiation and cytochemistry**

Cells at early passages cultured in complete MEF medium were placed in lineage-specific media for 2-3 weeks. For adipogenic differentiation, the medium of cells that were 2 days post-confluence was replaced with IMDM containing 100 μM indomethacin, 0.5 μM hydrocortisone, 0.5 mM 3-isobutyl-1-methyl-xanthine, 10 $\mu\text{g}/\text{mL}$ Insulin, and 10% calf serum for 2-3 weeks. Cells were stained with Oil Red O for intracellular fat droplets. For osteogenic differentiation, cells were treated with media containing 0.2 mM ascorbic acid, 10 mM beta-glycerophosphate and 0.1 μM dexamethasone, at 80% confluency. Osteoblastic phenotypes were observed over a 2-3 week period and examined by histochemical staining with alizarin red for calcium deposition, alcian blue to visualize proteoglycans, or for alkaline phosphatase activity. For myogenic differentiation, post-confluent cells were cultured in media containing reduced serum (2% calf serum) for 2-3 weeks. Cell morphology was documented with nuclei visualized by 4',6-diamidino-2-phenylindole (DAPI) staining and by indirect immunofluorescence for a muscle cell specific marker, smMHC.

Reverse transcription and quantitative PCR

Total RNA was isolated and reverse transcription (RT) was carried out with an RNeasy RNA extraction kit (Qiagen) and iScript cDNA synthesis kit (Bio-Rad) following the manufacturers' protocols. Briefly, for a 20 μ L RT reaction, 1 μ g of total RNA was mixed with 4 μ L of 5x iScript reaction mix, and 1 μ L of iScript Reverse Transcriptase, incubated at 25°C for 5 min, followed by extension at 42°C for 30 min and heat inactivation for 5 min at 85°C. Quantitative polymerase chain reaction (PCR) was carried out using an iCycler real-time PCR system (BioRad). Each 20 μ L reaction mix contained 10 μ L SYBR Green supermix (Biorad), 5 μ L containing 10 pmol of primer pair mix, and 5 μ L of diluted cDNA template (1:10) from the RT-PCR reaction. PCR reaction mixtures were heated at 95°C for 3 min, followed by 45 cycles of amplification (95°C for 10s; 60°C for 30s; 72°C for 30s). A final extension step was performed at 72°C for 10 min. Amplification results were analyzed using iCycler software (iQ5 multicolor optical v2). All primers were identified using the PrimerBank database (1).

Immunofluorescence

Cells were harvested by trypsinization, re-suspended at 10^7 cells/mL in FACS buffer (0.1% bovine serum albumin (BSA) and 0.1% sodium azide in PBS). The use of trypsin as a disaggregation method did not affect the expression pattern of most of the surface proteins observed. Conjugated primary antibodies (1 μ L) were added to 100 μ L aliquots of cells in a V-bottom 96-well micro plate, incubated for 40 min on ice, washed twice with FACS buffer and re-suspended in 200 μ L for cytometry (FACSCalibur, BD Biosciences) following the manufacturers' instructions. For multicolor flow cytometric analysis, cells were exposed to fluorochrome-conjugated antibodies recognizing CD54 (Pacific blue), Sca-1 (BV-510), CD73 (BV-605), CD80 (BV-650), CD24 (PE-CF594), CD140a (PE), CD71 (PE/Cy7), CD38 (PE/Cy7), CD120a (APC), CD107a (APC-Cy7), CD146 (APC), and CD90.1 (AF-700) in various combinations and fixed samples were analyzed on a FACS-Aria (BD Biosciences) at the Harvard Stem Cell Institute core facility. For multicolor flow cytometry of fibroblasts from embryonic organs, extracted organs were minced into small pieces and digested using Liberase™ DL collagenases

(Roche) and DNase I (Roche) in Hanks' balanced salt solution (HBSS, 138 mM NaCl, 5.33 mM KCl, 1.26 mM CaCl₂, 4 mM NaHCO₃, 0.3 mM Na₂HPO₄, 0.44 mM KH₂PO₄, 0.5 mM MgCl₂, 0.41 mM MgSO₄, 5.6 mM glucose) by incubating for 20-30 minutes in a CO₂ incubator at 37°C. Digested tissues were passed through a 100 µm mesh to obtain single cell suspensions. Fc receptors were blocked and cells were stained for flow cytometric analyses. A complete list of antibodies is presented in Table S7.

Confocal microscopy

To visualize intracellular proteins, cells were seeded in chamber slides (BD Falcon) and grown to 60-80% confluence. Cells were then fixed with 4% paraformaldehyde in PBS for 20 min, permeabilized and blocked with 0.1% Triton X-100 in blocking solution (0.2% bovine serum albumin in PBS) for 1 hour, and incubated with primary antibodies for 1 hour at room temperature. Cells were washed 5-6 times by PBS and further incubated with AF594 conjugated corresponding secondary antibodies (Invitrogen) for 45 min, and washed 6-8 times with PBS. The cells were mounted in mounting medium containing DAPI (Vector Laboratories) to stain nuclei, viewed and imaged using a Leica SP5 AOBS scanning laser confocal microscope and LAS AF Lite software. For FAP α staining, cells were permeabilized to improve the sensitivity. Antibodies are listed in Table S7.

***In vitro* collagen gel contraction assay**

Cells were trypsinized and re-suspended in Dulbecco's modified Eagle medium (DMEM) to 6 x10⁵ cells/mL, then mixed with an equal volume of 3 mg/mL rat collagen type I solution in pre-cooled tubes. 400-500 µL of cells were added to each well of a 24-well plate, using triplicate wells for each sample or a blank collagen gel control sample without cells. After polymerization for 30 min at 37°C, 0.5 mL of medium (DMEM+10% fetal bovine serum) was added and the cells were incubated for 4 hours in a cell culture incubator (37C, 5% CO₂). The medium was then changed to serum-free DMEM and the plate was incubated overnight. The following day the collagen gels were gently released from the underlying culture dish and the diameters of the gels were measured after 2-6 hours. The degree of collagen gel contraction was recorded as the average of the major and minor axes of the gel, and data were recorded as the percentage of initial gel area.

Measurements from 3 replicate wells were averaged and the standard deviations were calculated.

Single cell capture, transcript library preparation and sequencing

Multiple flow-sorted sub-populations were used for single cell mRNA sequencing. Growing cultures were dislodged using TrypLE™ (Thermo-Fisher) and cells were suspended at 250-500 cells/μL concentration. The cell suspension and Fluidigm C1™ suspension reagent were mixed at 3:2 ratios. 20 μL of mix was loaded onto a C1™ IFC. RNA extraction and mRNA amplification were performed for single cells in the C1™ micro-fluidics system using the Clontech SMARTer system and according to the manufacturers' recommendations. Amplified cDNA products were quantified by PicoGreen® (Thermo-Fisher) assay and adjusted to 0.1-0.3 ng/ml. cDNA products were prepared for sequencing using a Nextera XT-DNA sample preparation kit from Illumina. Up to 96 libraries were multiplexed per sequencing run.

Clustering and single cells gene expression data analysis

The R package Seurat (2) was used to generate cell population clusters. Principle component analysis was performed on genes present in at least 5 cells with an expression value of one count per million mapped reads. Ten statistically significant principal components were identified using a permutation test. Individual cells were projected based on their principle component scores onto a two dimensional plot using t-distributed stochastic neighbor embedding (t-SNE) (3). Violin density plots of gene expression levels for individual genes were generated using the Seurat package. Gene lists of the most variable expressed genes and of the best gene markers defining identified cell populations were generated.

Mouse cranial window preparation, implantation, and two-photon microscopy

All animal studies were conducted following protocols approved by the Institutional Animal Care and Usage Committee of Massachusetts General Hospital. Mouse cranial windows were prepared as described (4). In brief, mice were anesthetized using ketamine and xylazine and the head was fixed in a stereotactic frame. A disk of skin from the top

of the skull was removed after making a longitudinal incision between the occiput and the forehead. The periosteum was removed and a 6 mm circle was drawn over frontal and parietal regions of the skull. A groove was gradually grinded around the circle and the bone flap was separated from the dura mater while continuously rinsing the dura mater with sterile saline. Dura and arachnoid membranes were completely cut from both hemispheres using microscissors. Without damaging the sagittal sinus, unlabeled GFP-negative cells and GFP-labeled HUVECs were co-implanted in the center of the exposed region. A 7 mm round cover glass was fixed to the bone using cyanoacrylate glue. After several days the cranial windows were examined by two-photon microscopy using anesthetized mice immobilized in a stereotactic stage. Tetramethylrhodamine dextran was used to visualize newly formed vessels along with green HUVECs. In a separate set of experiments, co-implanted DsRed-labeled GFP-negative cells and unlabeled HUVECs were observed.

VEGFA Expression Analysis

One million cells were seeded in 100 mm culture plates and at day 3 media supernatants were replaced with medium containing 0.5% serum. Forty eight hours later culture supernatants were collected and centrifuged to discard any cell debris. An antibody cytokine array measurement was performed according to the manufacturer's instructions (RayBiotech). Biotinylated antibodies to cytokines were detected using IRDye-680 labeled streptavidin (Li-Cor Biosciences, Lincoln NE). The array was disassembled, washed, dried, and scanned using a Li-Cor Odyssey detector.

Supplemental References

1. Spandidos A, Wang X, Wang H, & Seed B (2010) PrimerBank: a resource of human and mouse PCR primer pairs for gene expression detection and quantification. *Nucleic acids research* 38(Database issue):D792-799.
2. Satija R, Farrell JA, Gennert D, Schier AF, & Regev A (2015) Spatial reconstruction of single-cell gene expression data. *Nature biotechnology* 33(5):495-502.
3. van der Maaten L, and Hinton, G. (2008) Visualizing Data using t-SNE. *J. Mach. Learn. Res.* 9:2579–2605.
4. Brown E, Munn LL, Fukumura D, & Jain RK (2010) In vivo imaging of tumors. *Cold Spring Harbor protocols* 2010(7):pdb prot5452.

Supplemental Figure Legends

Fig. S1. Primary fibroblasts from VEGF-GFP transgenic embryos.

Fibroblasts from the VEGF-GFP mouse embryos at stages E12.5 and E18.5 were isolated and cultured as described in Materials and Methods. (A) Fibroblasts from E12.5 embryos at passage 28 (1) or from E18.5 embryos at passage 30 (2) were analyzed by phase contrast microscopy. (B) A cytokine assay was performed on culture supernatants of GFP-positive and GFP-negative cells as described in SI Materials and Methods. GFP-positive cells showed higher levels of VEGFA compared to GFP-negative cells.

Fig. S2. ES cell and NIH3T3 fibroblast expression of antigens used to assess multipotency potential.

Wild-type mouse ES cells or NIH3T3 fibroblast cells were cultured in chamber slides (BD Falcon) for 1-2 days before fixation and permeabilization. Antigens were visualized by indirect immunofluorescence using antibodies to Fra-1, Pax-7, Nanog, Klf-4, NST, cMyc, Nestin, Cox-2, Sox-2, and Oct-4 as described in SI Materials and Methods. Images acquired with a Leica SP5 AOBS confocal microscope show antibody (red), and DNA (blue) as well as merged images. All antigens are present in ES cells (A), but not NIH3T3 fibroblasts (B). NIH3T3 fibroblasts express only NST and Fra-1.

Fig. S3. Phenotypic comparisons of GFP-negative and GFP-positive cells.

GFP-negative and positive cells from E18.5 VEGF-GFP transgenic mice were sorted for GFP expression, cultured in chamber slides (BD Falcon) and grown to 60-80% confluence before fixation and permeabilization. (A and B) Expression of pluripotency markers. GFP-negative and positive cells show a nucleolar specific staining for NST, nuclear staining for Fra-1, and an intermediate filament specific staining for Nestin. Expression of NST and Nestin was higher in GFP-negative cells whereas Fra-1 expression was higher in GFP-positive cells. Most of the ES-specific markers, (Oct-4, cMyc, Sox-2, Pax-7, Cox-2, Klf-4, and Nanog) were absent from both cell types. Images

were acquired with a confocal microscope, and color coded by antibody reactivity (red), DNA content (blue), and GFP presence (green).

Fig. S4. Localization of fibroblast, contractile protein and intermediate filament antigens.

GFP-negative and positive cells from E18.5 VEGF-GFP transgenic mice were sorted for GFP expression, cultured in chamber slides (BD Falcon) and grown to 60-80% confluence before fixation and permeabilization. (A and B) Cells were visualized by indirect immunofluorescence with antibodies recognizing sM22 α (*Tagln*), α SMA (*Acta2*), desmin (*Des*), vimentin (*Vim*), smMHC (*Myh11*), ER-TR7, and FAP α as described in SI Materials and Methods. GFP-negative cells express myofibroblast antigens (sM22 α and α SMA), the mesenchymal cell antigen vimentin and the fibroblast antigen FAP α , but not the myofibroblast and mature muscle cell antigens desmin and smMHC. GFP-positive cells express the ER-TR7 antigen but GFP-negative cells do not (Fig. S4B).

Fig. S5. Phenotypic characterization of colonies from E18.5 embryonic fibroblast-like cells.

(A) Colonies show normal morphology by phase contrast microscopy. (B) Flow-cytometric analyses of GFP expression by clones. Three clones, A6, B3, and D1 express GFP.

Fig. S6. Multipotency of cells from single colonies

Quantitative RT-PCR analyses of cells expanded from single colonies and exposed to media inducing differentiation into three lineages. The expanded cells exhibited varying degrees of susceptibility to the inducing media.

Fig. S7. FAP α expression identifies a subpopulation of cells from embryonic organs.

Fibroblast-like cells were identified by anti-FAP α reactivity. Single cell suspensions were prepared from E18.5 embryo organs. The cells were treated with Fc γ RII/RIII block and stained with FAP α antibody. Cells were washed three times and incubated with donkey

anti-rabbit secondary antibody. Cells were washed, fixed, and subjected to flow-cytometry. All organs contained anti-FAP α reactive cells.

Fig. S8. FAP α expression by fibroblasts cultured from embryonic organs.

Fibroblast-like cells were expanded from multiple embryonic organs in culture. The cells were stained with anti-FAP α antibody. Fibroblast populations from most of the organs were almost entirely FAP α positive. Fibroblasts from heart tissue contained a significant population that did not express FAP α . Red, isotype control; blue, anti- FAP α .

Fig. S9. Phenotypic diversity within fibroblasts cultured from embryonic organs.

Preparations of fibroblasts derived from 13 embryonic organs were incubated with CD24 (PE-CF594) and CD120a (APC) antibodies and analyzed by flow cytometry. The data were analyzed using FlowJo software. Substantial heterogeneity was observed among the analyzed populations.

Fig. S10. Histochemistry and RT-PCR analysis of GFP-negative cells.

Cells induced to differentiate were examined by cytochemistry using specific dyes, by reactivity with anti-smMHC antibody and by qRT-PCR as described in SI Materials and Methods. (A) Adipogenic, osteogenic, and myogenic differentiation of GFP-negative and GFP-positive cells. Panel 1 and 5, Oil Red O staining for fat droplets in cells exposed to adipogenic or conventional medium. Panels 2-4 and 6-8, staining with alcian blue, alizarin red or for alkaline phosphatase activity in cells exposed to osteogenic or conventional medium. Panel 9, myogenic differentiation of GFP-negative cells visualized with an antibody recognizing smMHC. (B) qRT-PCR analyses of GFP-negative and GFP-positive cells from E12.5 and E18.5 embryos undergoing *in vitro* differentiation. For myogenic induction, cells were exposed to myogenic induction or conventional medium and qRT-PCR was performed for smooth muscle-specific markers sm22 α (*Tagln*), smMHC (*Myh11*), desmin (*Des*), vimentin (*Vim*), α Tropomyosin (*Tpm1*), α SMA (*Acta2*), and caldesmon (*Cald1*). GFP-negative cells exposed to induction medium express elevated levels of these markers (B, 4 and C, 4). For osteogenic induction, cells were exposed to osteogenic induction or conventional medium. GFP-negative fibroblasts

showed a robust increase in the abundance of *runx2* (*Runx2*), osteocalcin (*Bglap*), osteonectin (*Sparc*), osteopontin (*Spp1*) and alkaline phosphatase transcripts (*Alpl*) (*B*, 5 and *C*, 5). The abundance of these transcripts in GFP-positive cells was unchanged (*B*, 2 and *C*, 2). For adipogenic induction, GFP-negative and GFP-positive fibroblasts were exposed to adipogenic or conventional medium and analyzed by qRT-PCR. The transcript abundance of aP2 (*Fabp4*), CEBP α (*Cebpa*) and PPAR γ (*Pparg*) genes increased in GFP-negative cells (*B*, 6 and *C*, 6) compared to GFP-positive cells (*B*, 3 and *C*, 3).

Fig. S11. Flow cytometric analyses of GFP-negative cells.

Cytometric analyses of GFP-negative cells for a panel of cell surface markers following differentiation into three lineages. Flow sorted and expanded GFP-negative cells were differentiated into osteogenic, myogenic, and adipogenic lineages in the respective induction media. Surface markers were analyzed by flow cytometry for differentiated cells (blue) and compared to undifferentiated cells (red). Expression of CD44, CD80, CD120a, and CD121 was reduced in all cases. Expression of CD24, CD38, and CD106 was reduced in some conditions whereas CD29, CD90.1, CD140a, Sca-1, and PDPN were little affected. CD36 expression appeared following adipogenic differentiation.

Fig. S12. Smooth muscle cell phenotype of GFP-negative cells.

(A) Light micrographs of GFP-negative cultures labeled by expression of dsRED visualized by phase contrast (1) or in the red channel (2). (B) *In vitro* collagen contraction was measured as described in SI Materials and Methods. A 24-well plate with 200,000 or 400,000 cells/well cultured inside 1.5% collagen gels for 24 h is shown. The adjacent graph shows the calculated change in area of the collagen gel. GFP-negative cells contracted collagen gels whereas GFP-positive cells did not. (C) Morphologies of cells cultured in the Matri-gel SMC culture system (BD Biosciences) in induction media for 2 days. Differentiated smooth muscle morphologies were observed for E12.5 cells from VEGF-GFP embryos (1), and 10T1/2 cells (2). The GFP-positive subpopulation from the E18.5 cells at passage 6 (3) or 34 (4) did not show smooth muscle morphology. (D) Cells were cultured in Matrigel (BD Biosciences) in induction medium for 2 days.

Immunofluorescence analysis of smooth muscle specific caldesmon (SM caldesmon) was performed as described in SI Materials and Methods. Images are of WT-FVB-E12.5 (1, 2) and C3H10T1/2 (3, 4).

Table S1. Similarities of GFP-positive and GFP-negative populations from E18.5 day fibroblast-like cells.

CD	GFP (+)	GFP (-)	CD	GFP (+)	GFP (-)	CD	GFP (+)	GFP (-)
3a	-	-	54	+	+	127	-	-
4	-	-	66a	+	+	133	-	-
9	+++	+++	71	+	+	135	-	-
11b	-	-	73	+	+	140a	++	++
14	+	+	80	++	++	144	-	-
18	-	-	81	++	++	146	++	+
19	-	-	86	-	-	150	-	-
24	+++	+++	88	-	-	196	-	-
29	+++	+++	90.1	+++	+++	202	-	-
30	-	-	90.2	-	-	226	-	-
31	-	-	96	-	-	309	-	-
34	+	+	105	+	+	Podoplanin	++	++
36	-	-	106	++	++	Tra-1-81	-	-
38	++	++	107a	+	+	Sca-1	+++	+++
44	++	++	117	-	-	SSEA-1, 3	-	-
45	-	-	120a	++	++	MHC-II	-	-
45R	-	-	121	++	++	DLL1, DLL4	-	-
48	-	-	122	-	-	FcεRI-α	-	-
49b, d	-	-	123	-	-	Pan NK cell	-	-

The CD or other antigens analyzed by flow cytometry are shown at left, with a scoring of expression intensity between – and +++.

Table S2. Fibroblast colonies from E18.5 VEGF-GFP transgenic mice.

150 mm Plates	Smaller Colonies (up to 1mm)	Bigger Colonies (>1mm)	Total number of Colonies	Efficiency (%)
1	32	8	40	0.80
2	29	3	31	0.62
3	41	6	47	0.94
4	40	7	47	0.78
5	54	8	62	0.83

$$\text{Cloning Efficiency} = \frac{\text{Total number of colonies}}{\text{Total number of cells seeded}}$$

Final colony formation efficiency: 0.8 %

Total number of colonies that could be transferred from 96-well plate: 34

Total colonies that could be expanded: 20

Number of GFP+ colonies expanded: 3

5000-7000 fibroblast-like cells isolated from E18.5 VEGF-GFP transgenic mouse embryo were plated in 150 mm cell culture dishes with complete MEF medium supplemented with 20% CS plus iron (Hyclone) and allowed to grow for 6-8 weeks with frequent changes of medium. Colonies were counted and the cloning efficiency calculated as described in the Materials and Methods.

Table S3. GFP-negative populations derived from single colonies *in vitro* exhibit heterogeneous cell surface protein expression patterns.

CD/ Clones	A1	A2	A3	A4	B1	B4	B5	B6	C1	C3	C4	C5	A6	B3	D1
14	+	-	+	-	-	+	+	+	-	+	+	-	+	-	-
18	-	-	-	-	-	-	-	-	-	-	-	-	-	-	-
24	+	-	++	+	+++	+++	+	+++	+++	+	+++	++	+	ND	++
29	+++	+++	+++	+++	+++	+++	+++	+++	+++	+++	+++	+++	++	+++	++
34	-	+	-	+	-	-	-	+	-	-	+	+	-	-	+
38	-	+	++	+	+	++	++	+	++	+	+	+	+	ND	+
44	++	++	++	++	++	++	++	++	++	++	++	++	++	++	++
54	+	ND	ND	+	ND	-	+	ND	-	-	+	-	-	-	-
66a	-	+	+	ND	+	++	+	+	+	ND	+	+	+	ND	+
71	+	+	+	+	+	+	+	++	+	+	+	+	-	+	-
73	-	-	-	-	+	-	-	+	-	-	-	-	-	-	-
80	+	+	+	+	+	+	+	++	+	++	+	+	+	+	+
81	+++	+++	+++	+++	+++	+++	+++	+++	+++	+++	+++	+++	+++	++	+++
86	-	-	-	-	-	-	-	-	-	-	-	-	-	-	-
90.1	-	+++	-	++	+++	+++	++	+	+	+	+++	+++	+	-	+
90.2	-	-	-	-	-	-	-	-	-	-	-	-	-	-	-
105	++	++	++	+	++	-	-	-	++	-	-	+	-	-	-
106	+++	+++	+++	+++	+++	+++	+++	+++	+++	+++	+++	+++	++	++	++
107a	+	+	++	ND	+	+	+	++	+	ND	ND	+	+	ND	+
117	-	-	-	-	-	-	-	-	-	-	-	-	-	-	-
120a	+	+	+	++	+	+	+	+	+	+	+	+	+	+	-
140a	+	+	++	++	++	+	++	+	++	+	++	+	+	+	+
Sca-1	+++	+++	+++	+++	+++	+++	+++	+++	+++	+++	+++	+++	+++	+	++
PDPN	++	+	-	+	+	++	-	+++	-	++	+	++	+	ND	+

Qualitative reactivity summary (ND) Not Determined.

Table S4. Genes shown in heat map

Cwc22	Msr1	Crip1	Al607873	Tlr8	Glpr1	Ccl12
Adgre1	Myo1f	Gmfg	Evi2a	Casp1	Ifi2712a	Cd72
Alox5ap	Ncf4	Hpgds	Il10rb	Cyth4	Rassf4	Tmem104
C3ar1	Nckap1l	Lat2	Ehd4	Dok2	Cx3cr1	Bin2
Capg	Pira6	Ms4a7	Sec11c	Hmha1	Pkib	Aif1
Ccl3	Pirb	Blnk	Unc93b1	Lair1	Rhog	Ptpn18
Cd14	Pld4	Btk	Slc7a8	Lrmp	Ncf1	Ifi30
Cd53	Plek	Clec4a2	Aldh3b1	Tlr7	Csf2rb	Irf8
Cd68	Ptprc	Coro1a	Lyn	Tnfaip8l2	Trpv2	Lgals9
Clec12a	Rac2	Fxyd5	Ctsb	Cybb	2610203C22Rik	Pik3r5
Clec4d	Rgs1	Lmo2	Grn	Dok3	Gpsm3	Prex1
Clec5a	Tmem106a	Srgn	Milr1	Dpep2	Rufy3	Mfap2
Ctss	Trem2	Blvrb	Prkcd	Sash3	Abhd12	15000150
Fcer1g	Tyrobp	C5ar1	Pon3	Shtn1	Mgat4a	10Rik
Fyb	Adam8	Ccl4	Adcy7	Tlr13	Dgkz	Sod3
Id2	Ccl9	Ctsc	Cxcl16	Wdfy4	Man2b1	Emb
Itgam	Cfp	Efhd2	Lgals3	Fli1	Emilin2	Agtr2
Laptm5	Cyba	Gcnt1	Plxnc1	Lpxn	Lipa	Srpx
Cwc22	Gp49a	H2-D1	Psmb8	P2ry6	Zfp710	Itm2a
Adgre1	Lilra6	Igsf6	Smpdl3a	Slc37a2	Tep1	Sfrp2
Alox5ap	Mpeg1	Fcgr2b	Ms4a6c	Atf3	Cd93	Nov
C3ar1	Nrros	Gpr137b-ps	Lgmn	Il2rg	Hhex	Thbs2
Capg	Pf4	Sirpa	Cd84	Lst1	Gpr137b	Tnfaip6
Ccl3	Ptpn6	Gatm	Csf2ra	Pik3cg	Arhgef6	Wdr62
Cd14	AF251705	1110007C09Rik	Gusb	C1qc	Cndp2	Ccl2
Cd53	Cd37	Arhgap30	Ninj1	Nfam1	H2-K2	Polq
Cd68	Cotl1	H2-K1	Rgs2	Slc27a1	Psmb10	Mxd3
Clec12a	Csf1r	Al662270	Anpep	Glul	Elmo1	Ccnf
Clec4d	Ctsz	Lcp2	Creg1	BC005537	Samhd1	Actg2
Clec5a	Dab2	Apobec1	Ucp2	Ncf2	Sp110	Ecscr
Ctss	Fcgr3	Itgb2	Slc43a2	Pid1	Arhgap9	Brip1os
Fcer1g	Fermt3	Ms4a6b	Ppm1h	Pip4k2a	Ikzf1	E2f7
Fyb	Lyz1	Cadm1	Bhlhe41	Cxcr4	Cd200r1	Mcm10
Id2	Lyz2	Mafb	Adap2	Itga6	Grb2	Rbl1
Itgam	Pira2	Syk	Spi1	Trim30a	Hcls1	Gm16702
Laptm5	Plin2	Blvra	Dock2	Mrc1	Arl11	Lcmt2
Lcp1	Slnf2	Nceh1	Fxyd2	Irf5	Fmnl1	Gm10190
Lilrb4	Stab1	Ctsd	Inpp5d	Rgs10	Myo1g	Prelp
Ms4a6d	Cd36	H2-Q2	Stom	Arrb2	Oas1a	

Table S5. Highly variable genes in single cell analysis.

1110032A03Rik	Adgrd1	C1qa	Col5a3	Eid3	Igf2bp1
1600010M07Rik	Adgre1	C1qb	Coro1a	Elf1	Igfbp3
1700024P16Rik	Adgrg2	C1qc	Cox5b	Elf4	Igfbp5
1700093K21Rik	Adipoq	Cables2	Cpeb1	Elmo1	Irf2bpl
1810022K09Rik	Adipor2	Cadm1	Cpeb2	Enho	Irf3
2010315B03Rik	Agbl3	Camta2	Cpeb3	Enox2	Itga7
2210408F21Rik	Agfg2	Car3	Cpsf4	Erich5	Itrip12
2310039H08Rik	Agpat2	Ccdc136	Csf1r	Ero1l	Jade3
2410015M20Rik	Agps	Ccl12	Csrnp1	Etfa	Jazf1
2610507I01Rik	Ahdc1	Ccl3	Ctcf	Evc	Kat6b
2700099C18Rik	Akap17b	Ccl4	Ctsh	Evi5	Kctd6
2810417H13Rik	Aldh3b2	Ccl6	Cul7	Exoc2	Kdm6b
2900060B14Rik	Aldh3b3	Ccny	Cx3cr1	Exoc5	Kif13a
3300005D01Rik	Amacr	Ccr1	Cxadr	Exoc8	Kif1a
4921504A21Rik	Amotl2	Ccr12	Cxcl2	F13a1	Kif3a
4930427A07Rik	Anapc13	Cd2bp2	Cybb	Fabp3	Kif4
4930431F12Rik	Anapc2	Cd36	Cyp2j9	Fabp4	Kiz
4930512M02Rik	Ankrd13a	Cd48	D830005E20Rik	Fahd2a	Klhdc10
4933400A11Rik	Ankrd16	Cd72	Dagla	Fam111a	Klhdc3
4933400F21Rik	Ap4e1	Cd74	Dars	Fam122b	Klhl2
6330416G13Rik	Apbb3	Cdkn1c	Dcun1d5	Fam129a	Klhl5
6330549D23Rik	Apoe	Cenpb	Ddt	Fam133b	Kpna4
9330158H04Rik	Apol6	Cenpw	Dennd4a	Fam160b2	Krtcap2
9430015G10Rik	Arap3	Cep128	Dgcr6	Fam172a	Lat2
9430037G07Rik	Arfgef2	Cfd	Dhx9	Fam43a	Lcn2
A230057D06Rik	Arhgap11a	Cfp	Dis3	Fancm	Lig1
A630020A06	Arl4c	Chd3	Dis3l2	Fbxo45	Lincppara
A830080D01Rik	Arpp21	Cherp	Dmpk	Fbxw8	Lipe
AI450353	Atg3	Chl1	Dmxl1	Fcgr2b	Lrch1
AU041133	Atp1a2	Chrdl1	Dnajc17	Fcgr3	Lrp10
AY512931	Atp2b4	Chrna1	Dnm1	Fcrls	Lrpprc
Abhd17b	Atp6v0a2	Chrnd	Dnm3	Fez2	Lrrc27
Acadsb	Atxn7l3b	Ciao1	Dnmbp	Fhod1	Lrrtm2
Acox1	Avl9	Cidec	Dok2	Firre	Luzp2
Acrbp	B3gat3	Clcn2	Dsel	Fkbp5	Lym5
Acsl1	Banp	Clcn7	Dus3l	Folr2	Lym9
Acsl5	Bard1	Clic4	Dusp16	Frmd4b	Lyz1
Acta1	Basp1	Cmas	Dut	Fzd3	Magohb
Actc1	Bet1l	Cnr1	Dzip3	G2e3	Malt1
Actr1b	Blzf1	Cntn1	E030024N20Rik	Gabbr1	Man2a1
Adam8	Brd9	Cog1	E2f5	Galnt10	Map2
Adgra2	Bri3	Col4a4	Egfl6	Gart	Mapkap1

March6	Nkd2	Plxna2	Tbc1d32	Ubtcd2
Mcidas	Nkiras1	Pnir	Tcof1	Ugt1a6a
Med15	Notch1	Pnpla2	Tenm3	Unkl
Meis3	Npat	Pnpla7	Tgfb1	Usp48
Mettl22	Npl	Pogk	Thg1l	Uxs1
Mfap1b	Nptx1	Pomgnt1	Timm10b	Vac14
Mib2	Npy	Pou2f1	Tktl1	Vat1
Mid1	Nrcam	Ppm1k	Tll1	Vegfc
Mkx	Nrk	Ppp1r2	Tln2	Vmn2r55
Mlec	Nrxn1	Ppp2r4	Tlr13	Vps37a
Mlph	Nt5c2	Pqlc1	Tmc4	Vps51
Mmp12	Numbl	Pqlc2	Tmed9	Vps53
Mmp16	Oasl2	Prex2	Tmem131	Vsig10l
Moxd1	Odc1	Prkd1	Tmem138	Wdpcp
Mpdz	Odf2	Prkd2	Tmem173	Wdr46
Mpeg1	Olfml2a	Prrc1	Tmem192	Wdr7
Mrap	Osbpl6	Psg29	Tmem203	Wfdc17
Mrc1	Palm2	Ptchd4	Tmem70	Wrnip1
Mrpl16	Pam	Ptges3l	Tmem8	Yod1
Mrpl36	Pan2	Ptpn4	Tmem82	Yrdc
Mrps31	Papola	Pus10	Tmem8c	Zbtb44
Ms4a7	Parp14	Pxdn	Tnfrsf1a	Zc3hav1
Mtm1	Pbk	Pycr1	Tnfrsf26	Zcchc5
Mtpap	Pcdh20	Rab20	Tnmd	Zdhhc1
Murc	Pcdhb17	Rad51	Tnni1	Zfand3
Mvk	Pcdhga8	Rad54l2	Tnnt2	Zfp35
Mxi1	Pcdhgc5	Ralgapb	Trak2	Zfp397
Myl1	Pcif1	Rarb	Trem2	Zfp462
Myo18a	Pcsk5	Rbm12	Trf	Zfp511
Myo1f	Pdlim7	Rdm1	Trim30a	Zfp608
Myog	Pdpc1	Reg1	Trim39	Zfp672
Myoz3	Pdzd7	Rel	Trmt12	Zfp715
Naalad2	Per2	Rep15	Trp53bp2	Zfp758
Napg	Phc1	Rer1	Trpm3	Zfp759
Ncf4	Phc3	Retn	Trps1	Zfp811
Nckap5l	Phf10	Rfx3	Tsen2	Zfp862-ps
Ndrp2	Phf2	Rlf	Tsga10	Zfp9
Ndufa3	Phyh	Rmnd5b	Tspan2	Zfp944
Ndufa5	Pigo	Rnf150	Ttc39b	Zhx2
Ndufb2	Pih1d1	Rnf166	Ttc7b	Zmym5
Ndufc2	Pik3c2a	Rnf19b	Ttn	
Neb	Plcb4	Syde2	U2af2	
Nes	Plekho1	Tbc1d12	Ube2d2a	
Ngfrap1	Plscr3	Tbc1d22a	Ubr2	

Table S6. Primers used for qRT-PCR.

Gene Name	F: 5'-3' R: 5'-3'
GAPDH	GGAGCCAAACGGGTCATCATCTC GAGGGGCCATCCACAGTCTTCT
sM22 α	ACCAAAAACGATGGAAACTACCG CATTGAAGGCCAATGACGTG
smMHC	AAGCTGCGGCTAGAGGTCA CCCTCCCTTTGATGGCTGAG
Desmin	GTGGATGCAGCCACTCTAGC TTAGCCGCGATGGTCTCATA
Vimentin	CTTGAACGGAAAGTGGAATCCT GTCAGGCTTGAAACGTCC
α Tropomyosin	AACGGTGACGAACAACCTTGAA GGAAGTCATATCGTTGAGAGCG
α SMA	GTCCCAGACATCAGGGAGTAA TCGGATACTTCAGCGTCAGGA
Caldesmon	GTACACCAATGCAATCGAGGG CCTTCTCCACATGCTCTTGA
sk-MLC2	TTCAAGGAGGCGTTCCTGTA TAGCGTCGAGTTCCTCATTCT
sk-Myogenin	CGGCCCTAACAAGAGGAG CAACATCACATCCCTTGGGAC
Runx2	GAGGCCGCCGCACGACAACCG CTCCGGCCCACAAATCTCAGA
Osteocalcin	CTGACCTCACAGATCCCAAGC TGGTCTGATAGCTCGTCACAAG
Osteonectin	ACTACATCGGACCATGCAAATAC GTACAAGGTGACCAGGACATTTT
Osteopontin	AGCAAGAACTCTTCCAAGCAA GTGAGATTCGTGAGATTCATCCG
Collagen I	GCTCCTCTTAGGGGCCACT CCACGTCTCACCATTGGGG
ALP	ATGGGCGTCTCCACAGTAAC CTGAGTGGTGTTCATCGC
aP-2	AAGGTGAAGAGCATCATAACCCT TCACGCCTTTCATAACACATTCC
CEBP- α	CAAGAACAGCAACGAGTACCG GTCACTGGTCAACTCCAGCAC
PPAR γ	TATGGAGTGACATAGAGTGTGCT CCACTTCAATCCACCCAGAAAG

Table S7. Antibodies used for confocal microscopy:

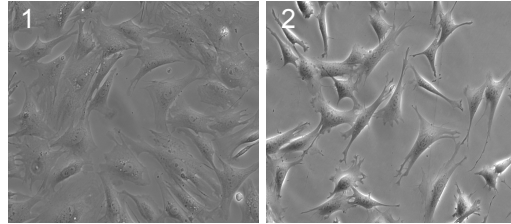
Antigen	Clone	Manufacturer	Catalog number	Lot number
Oct-4	C30A3	Cell Signaling	2840S	2
SM22 α	polyclonal	Abcam	ab14106	714669
FAP α	polyclonal	Abcam	ab53066	687932
FAP α	polyclonal	Abcam	ab28244	GR132121-8
cMyc	9E10	Abcam	ab32	685668
α SMA	1A4	Sigma-Aldrich	A5228	128K4843
ER-TR7	ER-TR7	Abcam	ab51824	764760
Nucleostemin	polyclonal	Abcam	ab32682	699588
Nestin	401	Abcam	ab11306	724974
Pax-7	EE-8	SantaCruz	sc81975	I2809
Fra-1	N-17	SantaCruz	sc183	I0809
Cox-2	33/Cox-2	BD	610203	42936
Nanog	M-17	SantaCruz	sc30329	H0609
Sox-2	H-65	SantaCruz	sc20088	H2109
Klf-4	T-16	SantaCruz	sc12538	E2909
smMHC	G-4	SantaCruz	sc6956	H0508
Desmin	RD301	BD	550626	32619
Vimentin	VIM-13.2	Sigma-Aldrich	V5255	068K4808

Antibodies used for flow cytometry:

Antigen	Clone	Manufacturer	Fluorescent dye	Catalog number	Lot number
CD4	GK1.5	Biologend	APC	100411	B161912
CD9	MZ3	Biologend	PE	124805	B124956
CD11b	M1/70	Biologend	APC	101211	B171230
CD14	Sa 14.2	Biologend	APC	123311	B155594
CD18	C71/16	BD	PE	553293	M054690
CD19	6D5	Biologend	PE	115508	B120253
CD24	M1/69	Biologend	APC	101813	B135111
CD29	HM \square 1-1	Biologend	APC	102215	B147686
CD30	mCD30.1	eBioscience	PE	12-0301-81	E016831
CD31	390	Biologend	APC	102409	B144752
CD34	HM34	Biologend	APC	128611	B146666
CD36	HM36	Biologend	APC	102611	B129606
CD38	90	Biologend	APC	102712	B148373
CD44	IM7	Biologend	APC	103011	B146670
CD45	30-F11	Biologend	PE	103105	B122071
CD48	HM48-1	Biologend	PE	103411	B130533
CD54	YN1/1.7.4	Biologend	APC	116119	B143429
CD66a	MAb-CC1	Biologend	PE	134505	B124593
CD71	R17217	eBioscience	PE	12-0711-81	E020852
CD73	TY/23	BD	PE	550741	37675
CD80	16-10A1	Biologend	APC	104713	B157138

Fig. S1

A



B

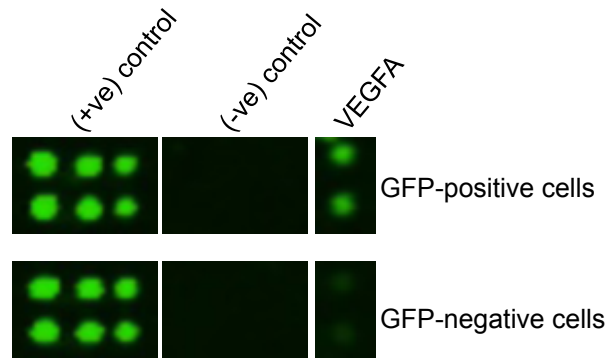
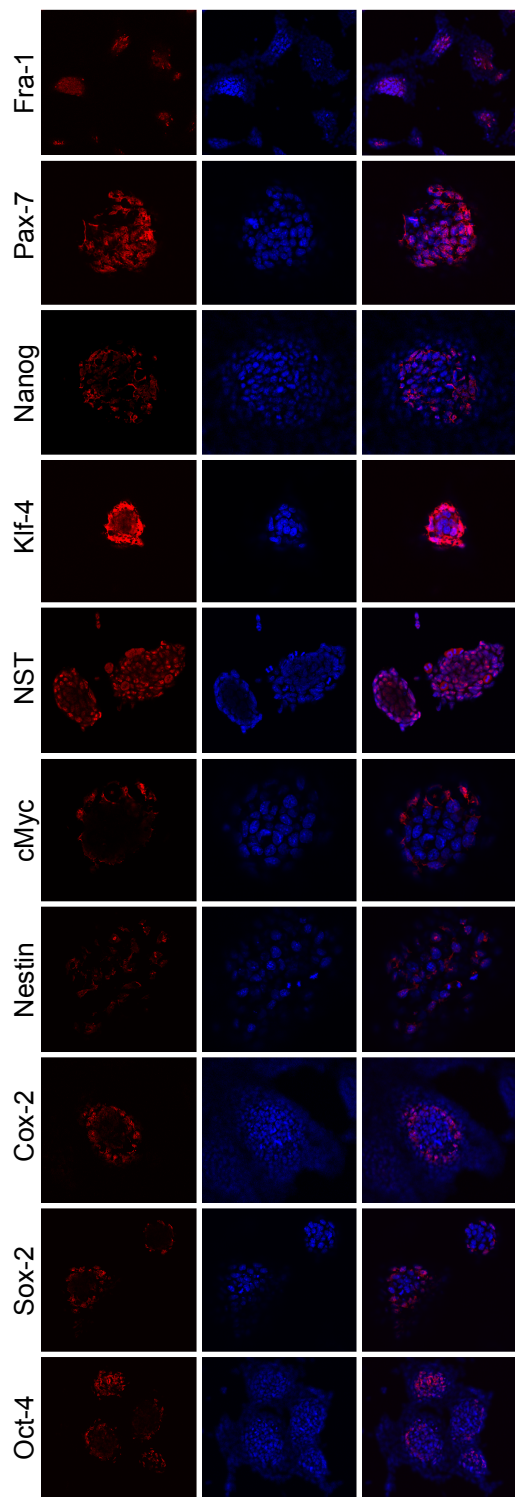


Fig. S2

A



B

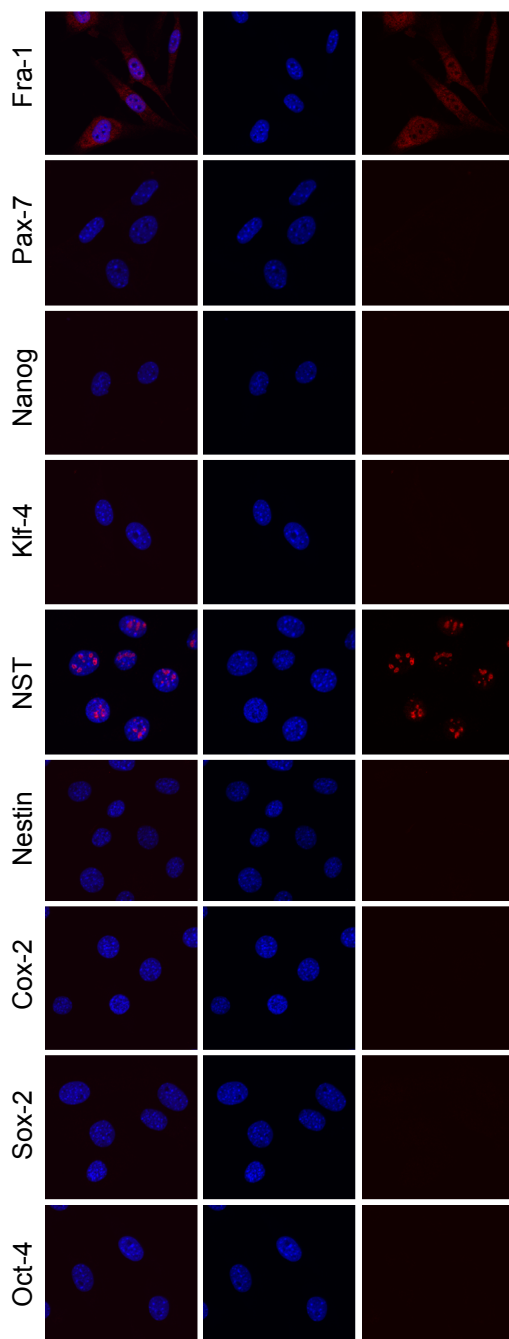
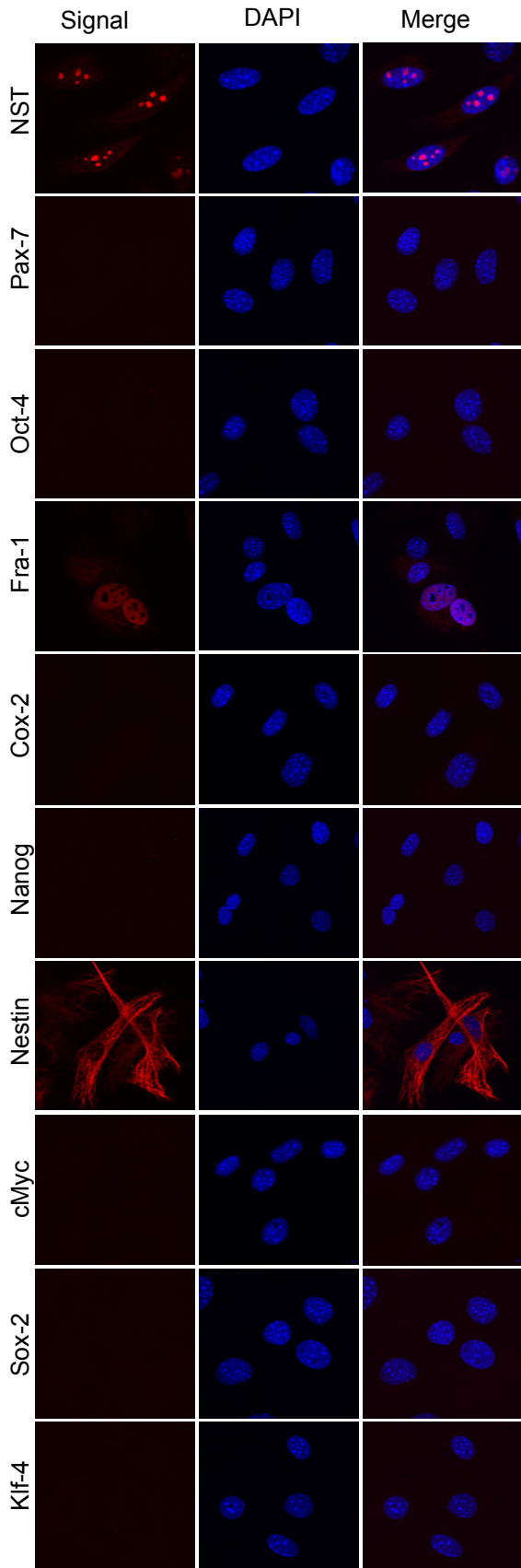


Fig. S3

A



B

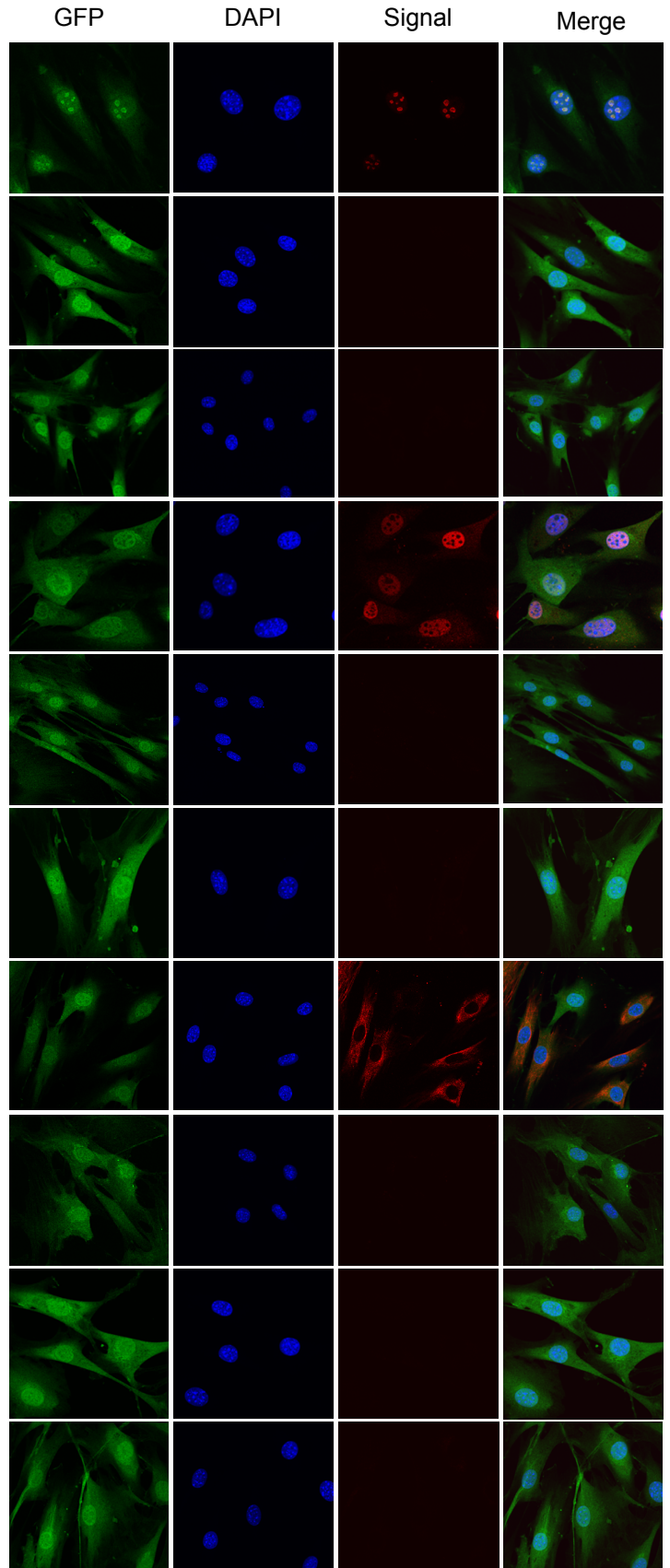
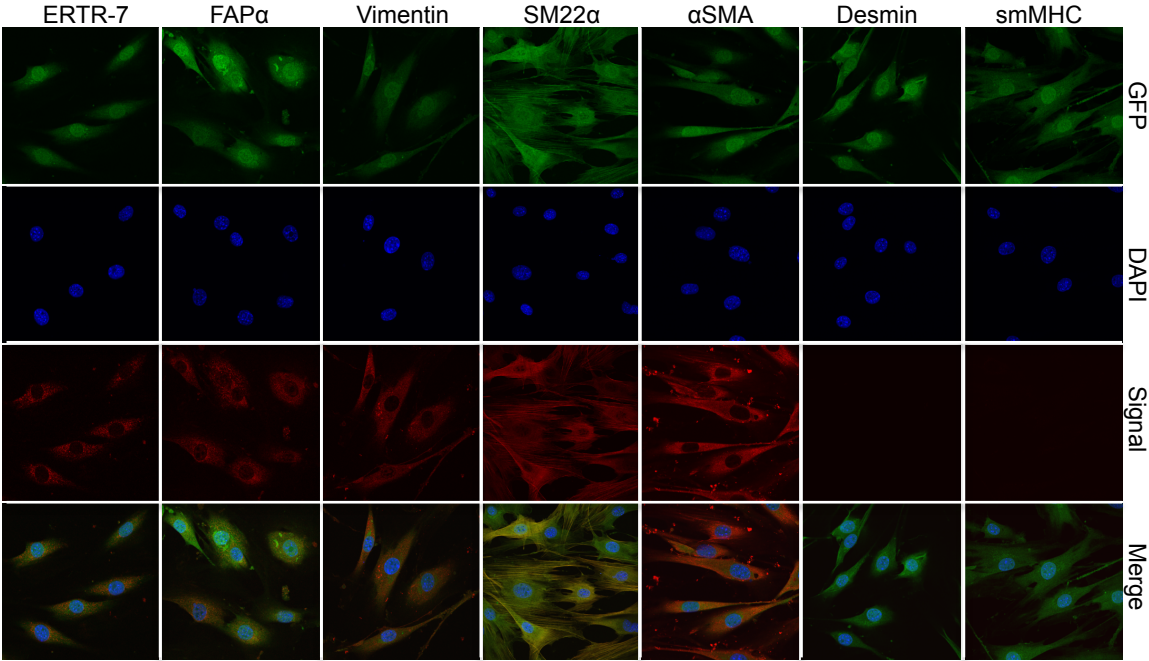


Fig. S4

A



B

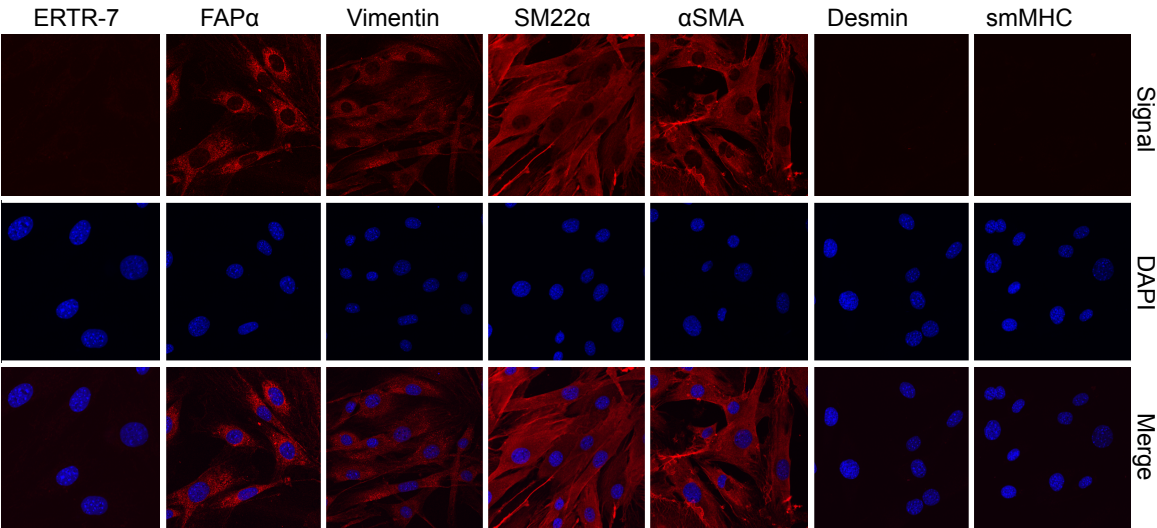
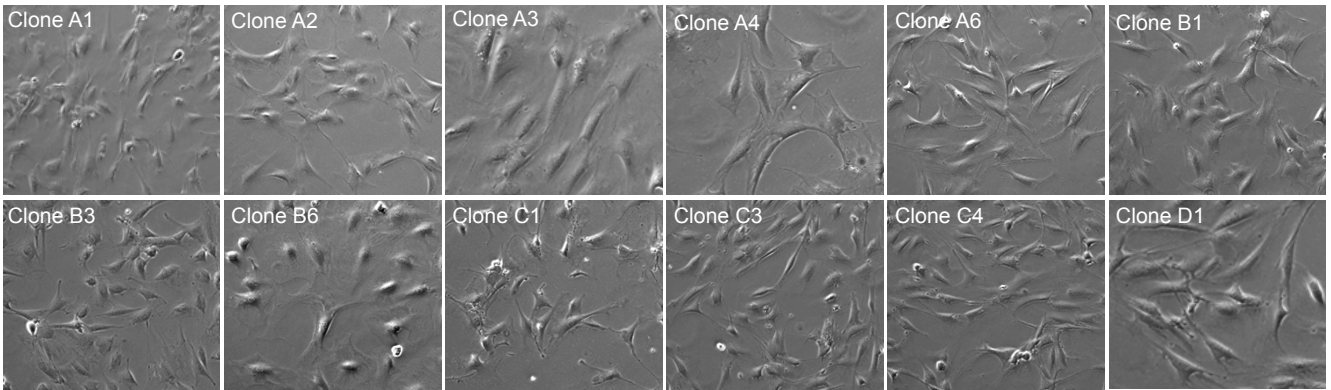


Fig. S5

A



B

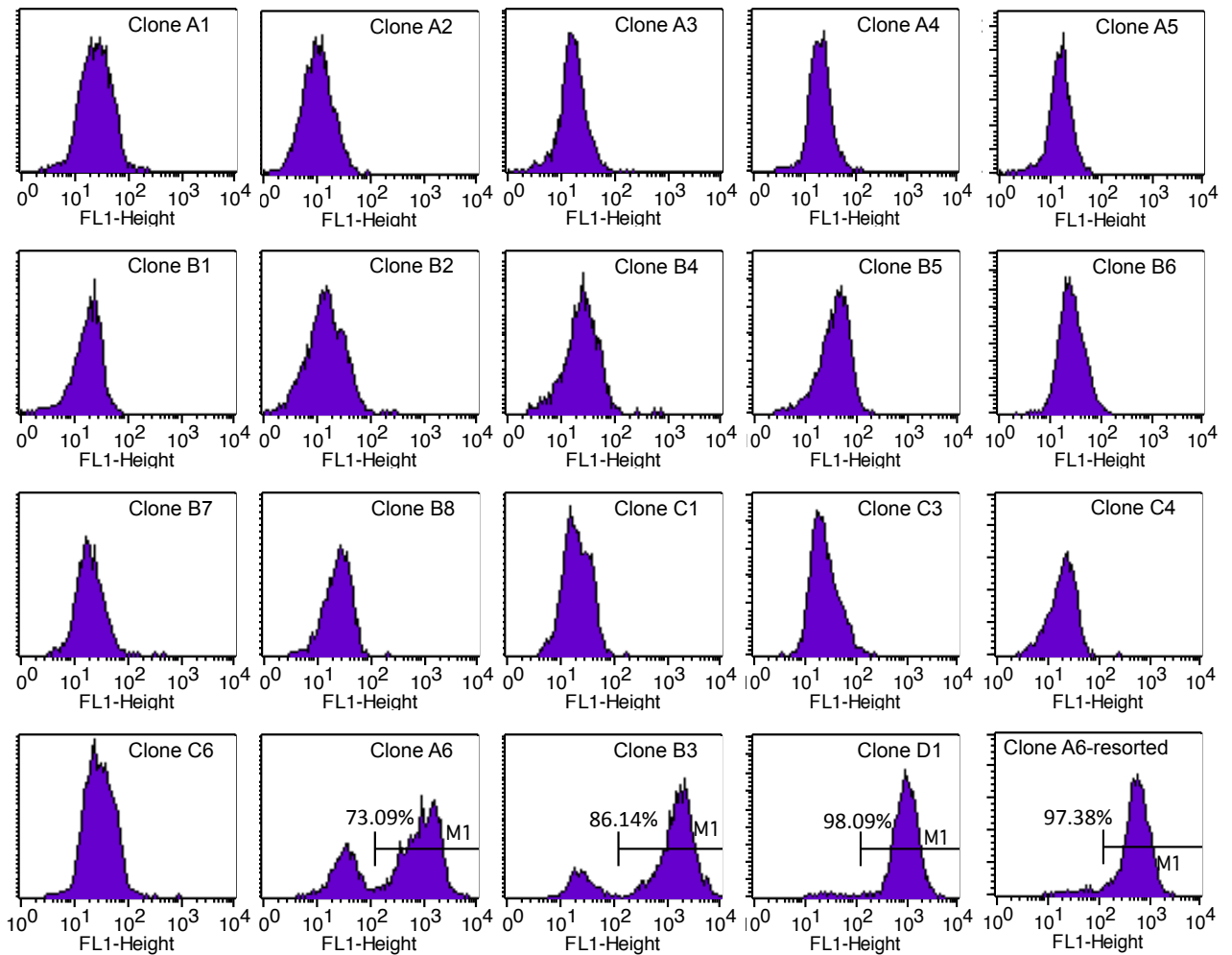


Fig. S6

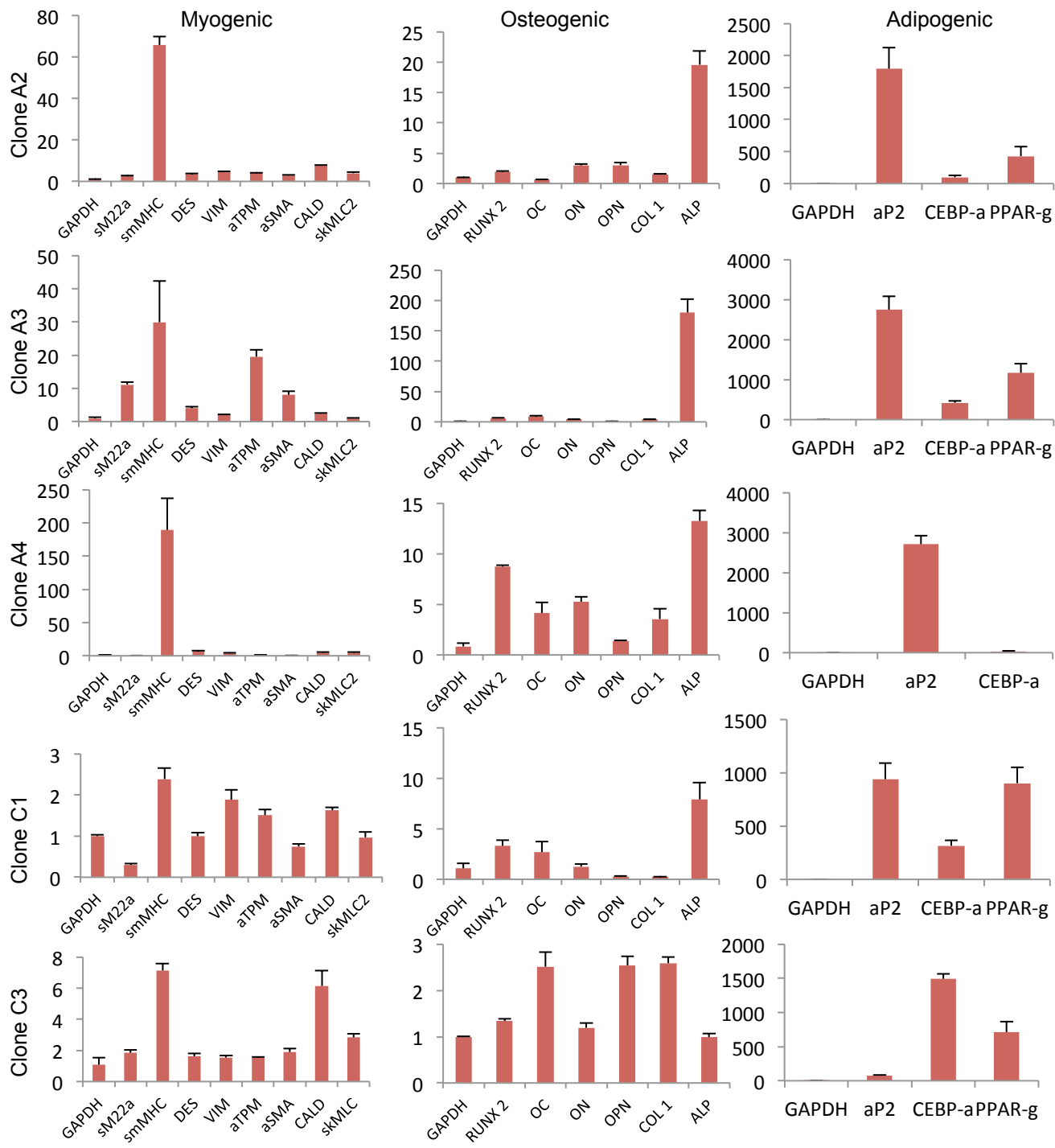


Fig. S7

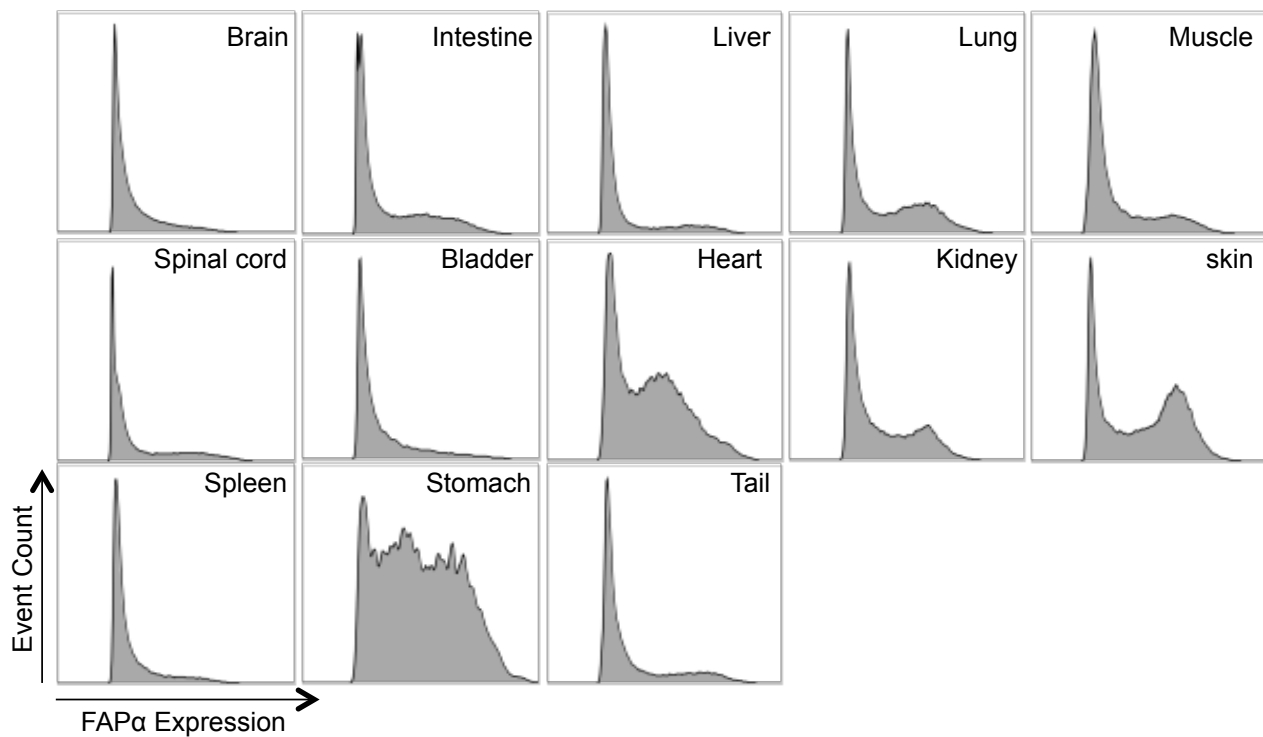


Fig. S8



Fig. S9

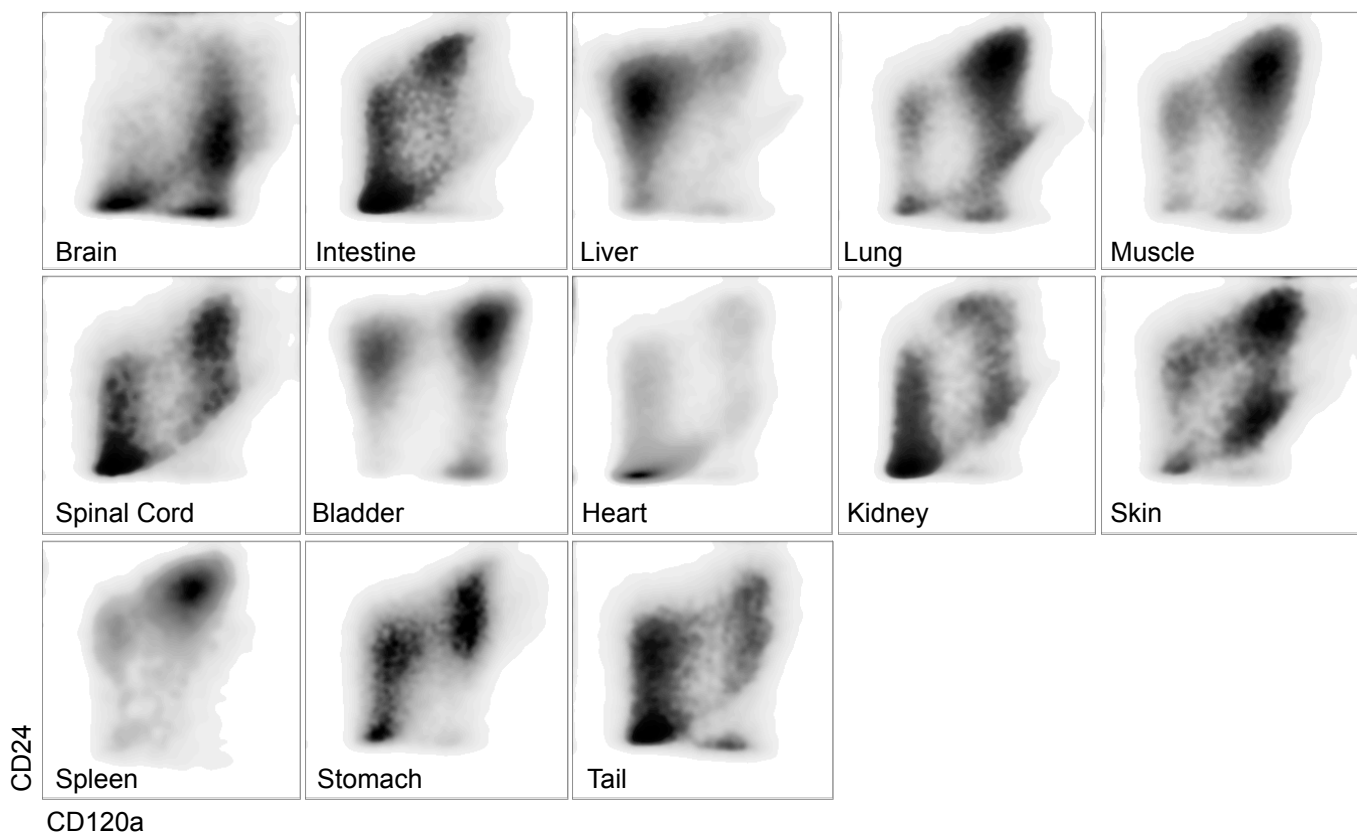


Fig. S10

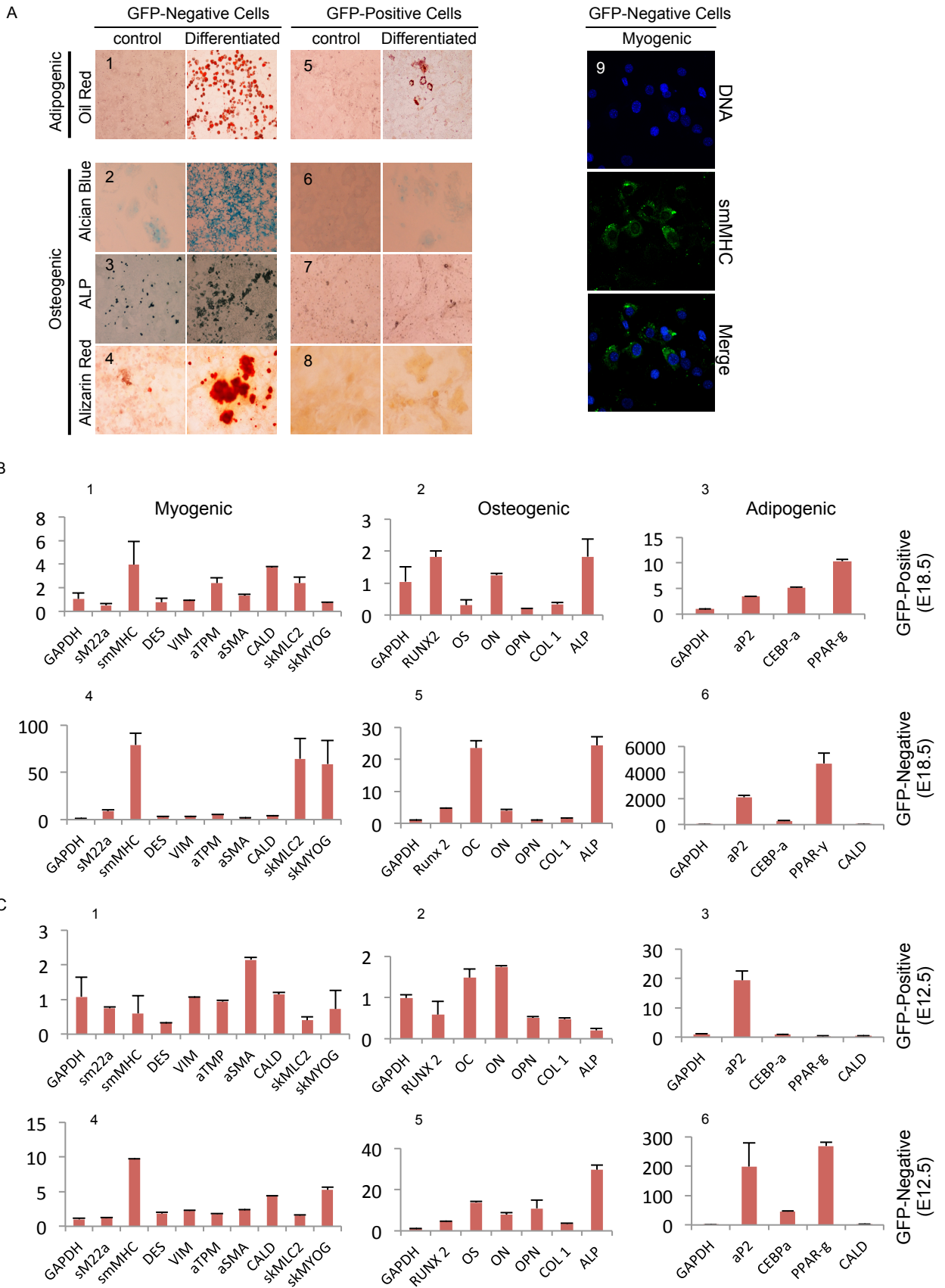


Fig. S11

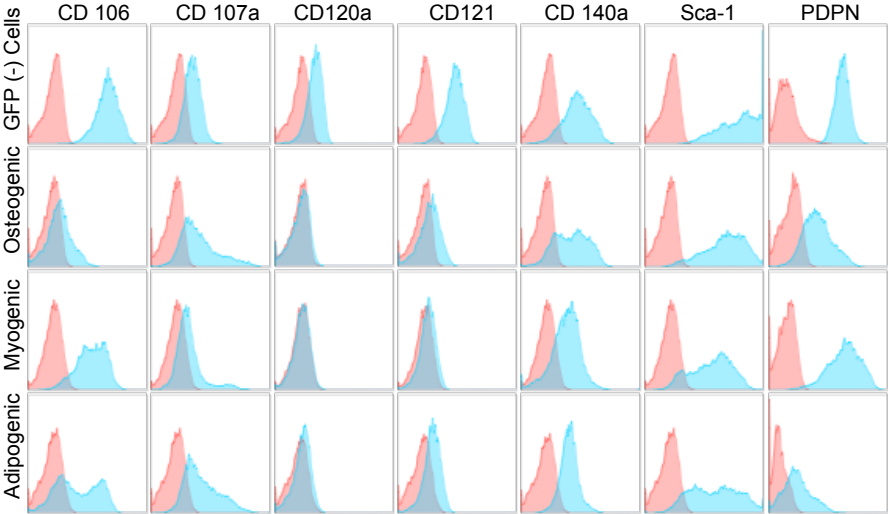
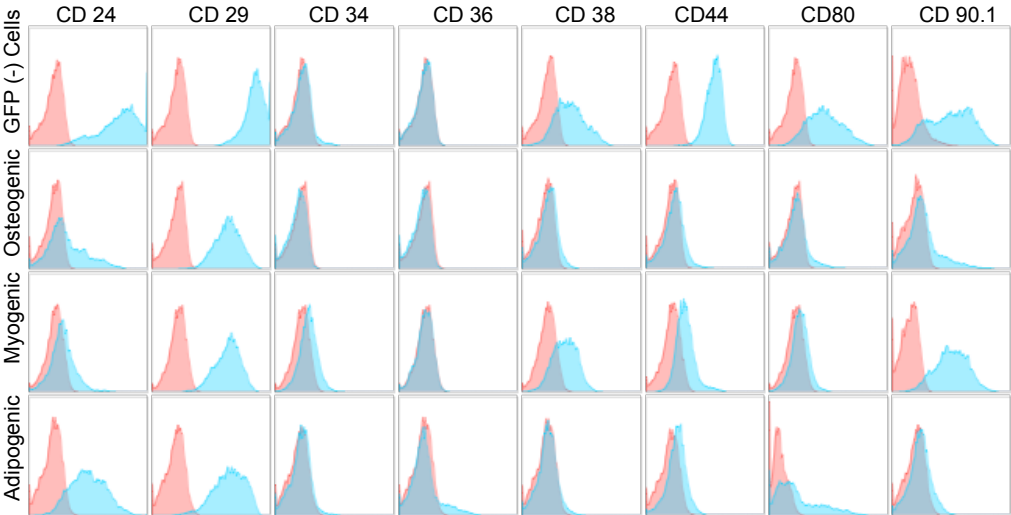
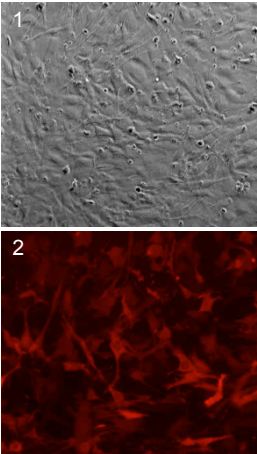
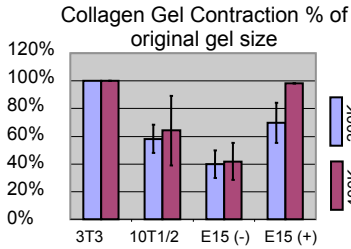
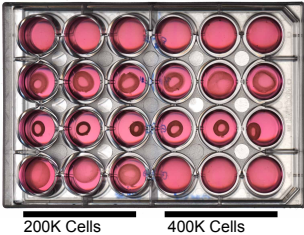


Fig. S12

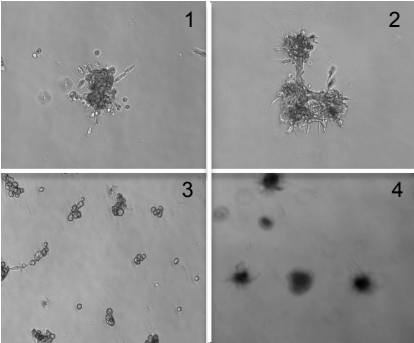
A



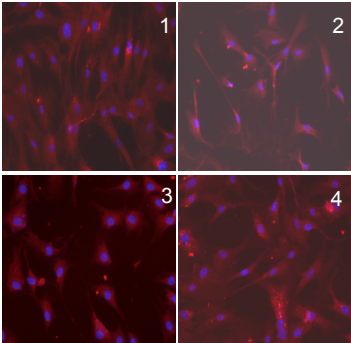
B



C



D



CD81	Eat-2	Biologend	PE	104905	B161589
CD86	GL-1	Biologend	APC	105011	B165162
CD88	20/70	Biologend	APC	135807	B141845
CD90.1	OX-7	Biologend	APC	202526	B142843
CD90.2	30-H12	Biologend	APC	105311	B141652
CD96	3.3	Biologend	APC	131709	B135887
CD105	MJ7/18	Biologend	APC	120413	B134487
CD106	429	Biologend	APC	105717	B136773
CD107a	1D4B	Biologend	APC	121613	B130800
CD117	2B8	Biologend	APC	105811	B147157
CD120a	55R-286	Biologend	APC	113006	B171052
CD121	JAMA-147	Biologend	APC	113509	B146865
CD122	5H4	eBioscience	PE	12-1221-81	E000616
CD123	5B11	Biologend	PE	106005	B168602
CD127	A7R34	Biologend	APC	135011	B142837
CD133	315-2C11	Biologend	APC	141207	B148289
CD135	A2F10	Biologend	APC	135309	B141174
CD140a	APA5	Biologend	APC	135907	B146656
CD144	BV13	Biologend	APC	138011	B145963
CD146	ME-9F1	Biologend	APC	134711	B182051
CD150	TC15-12F12.2	Biologend	APC	115909	B123557
CD202	TEK4	Biologend	APC	124009	B147798
CD226	10E5	Biologend	PE	128805	B121688
CD309	Avas12	Biologend	APC	136405	B142806
Podoplanin	8.1.1	Biologend	APC	127409	B139665
Sca-1	D7	Biologend	APC	108111	B140513
DLL1	HMD1-3	Biologend	APC	128313	B132325
DLL4	HMD4-1	Biologend	APC	130813	B142335
CD11c	N418	Biologend	APC	117309	B181249
CD54	YN1/1.7.4	Biologend	Pacific blue	116116	B183162
Sca-1	D7	Biologend	BV-510	108129	B199632
CD73	TY/11.8	Biologend	BV-605	127215	B189603
CD80	16-10A1	Biologend	BV-650	104731	B195752
CD140a	APA5	Biologend	PE	135906	B177404
CD38	90	Biologend	PE/Cy7	102718	B168859
CD107a	1D4B	Biologend	APC-Cy7	121616	B192509
CD90.1	OX-7	Biologend	AF-700	202528	B185299
CD71	R17217	BioLegend	PE/Cy7	113812	B169143
CD24	M1/69	BD	PE-CF594	562477	4192822